Journal of Computational Applied Mechanics 2026, 57(4): 615-638

DOI: 10.22059/jcamech.2026.421447.1937

RESEARCH PAPER

# 3-D Finite Element Stress Analysis of Lower-Limb Prosthetics with Different Composite Materials

O. Anwar Bég [a], Emily Branney [b], Tasveer A. Bég [c], S. Kuharat [a], M.M. Bhatti [d,e,*], Ali Kadir [a], Walid S. Jouri [a]

[a] *Multi-Physical Engineering Sciences Group (MPESG), Aeronautical and Mechanical Engineering Department, Corrosion and Coatings Lab, Room 3-08, SEE Building, University of Salford, Manchester, M54WT, UK*

[b] *PhD student (Silicon Doping For Solid State Quantum Technologies), Physics Department, SEE Building, University of Salford, Manchester, M54WT, UK. (formerly MSc Aerospace Engineering Programme)*

[c] *Engineering Mechanics Research, Israfil House, Dickenson Rd., Manchester, M13, UK*

[d] *Department of Physics, College of Science, Korea University, 145 Anam-ro, Seongbuk-gu, Seoul 02841, Republic of Korea*

[e] *Material Science Innovation and Modelling (MaSIM) Research Focus Area, North-West University (Mafikeng Campus), Private Bag X2046, Mmabatho 2735, South Africa*

**Abstract**

**This article studies a key area in modern biomechanical rehabilitation engineering-prosthetic design and numerical simulation. FEA stress analysis in ANSYS APDL/WORKBENCH is conducted for a robust geometry resembling a lower limb prosthetic inspired by the "Sara Diogo design". A parametric study of different loading conditions is conducted to both evaluate the suitability based on the current available prosthetics, and to critically evaluate the results against pre-existing studies to check validity. Carbon fibre (395 GPa), Epoxy Carbon Woven (395 GPa) Prepreg, and E-Glass are the 3 selected composite materials based on current practice in prosthetics design. SOLIDWORKS software is deployed to create robust and commercially pragmatic 3-D prosthetic geometries. Appropriate loading conditions are imposed. Static elastic stress analysis simulations are conducted for different materials. Mesh independence tests are also conducted, and tetrahedral (pyramidal) elements are deployed. Equivalent elastic stress, equivalent elastic strain, maximum principal stress and total deformation plots are presented for all three materials. Generally, all the materials demonstrate resilience although carbon fibre, while producing the highest von-Mises stress, does not yield and retains structural integrity, with maximum stresses computed never exceeding the yield strength. This could also be said for all composites, as they do not typically have a yield strength, the von-Mises stress will also be high. The relative cost/weight benefits of the different materials are also appraised. The study provides a good foundation for future refinement to consider impact dynamical, torsional and other complex loads relevant to prosthetic and orthotic design.**

**Keywords:** Lower-limb prosthetics; Finite element analysis; Carbon fibre; Epoxy Carbon Woven Prepreg; E-Glass; total deformation; ANSYS. 3-D stress modelling.

[*] Corresponding author. *E-mail address:* mmbhatti@korea.ac.kr

## 1. Introduction

As the global demand for prosthetics increases, so does the requirement for continued innovation in order to enable those who require the use of prosthetics to continue to move freely within the evolving word. There are many reasons as to why one may opt to use a prosthetic, including mobility, aesthetics, and a sense of returning to normalcy. Prosthetics and orthotics cover a vast range of problems, and each is unique to the user. There are key differences to establish before divulging into the current problems and ways to improve lower-limb prosthetics. Orthotics and prosthetics are not the same, although can be covered by the same departments in healthcare. An orthosis is a type of support/brace used to help those who still have their limb and need additional support, whereas a prosthesis is an artificial limb [1], used to replace a lost limb with the aim of supporting the patient and improving the quality of life. It is also important to recognise and define the two types of lower limb prosthetic, transfemoral (above the knee), and transtibial (below the knee). Comprehensive surveys of recent progress in design and analysis of lower-limb prosthetics have been presented by Andrysek [2] and Neelen et al. [3]. These have emphasized both laboratory prototype testing and the excellent capabilities of modern finite element computational packages in simulating and refining by a virtual approach, the resilience and comfort of modern prosthetics. Computational stress analysis studies are now an integral component of prosthetic design and are being used both to stress-test (with experiments) the abilities of new and emerging designs for prosthetic devices, as well as for optimizing and evaluating the effectivity of existing designs. Understanding how the devices function under stress can aid in highlighting areas of imbalance, which can be used to further develop prosthetics to improve user comfort and long-term compatibility [4]. Singh et al. [5] reviewed in detail a number of computer scanning and finite element simulations on lower limb prostheses. They highlighted the uses of CT scans to establish the specific geometry of the residual bones and limbs, in particular, the transtibial sockets of individuals. They showed that CT scans, alongside finite element analysis (FEA), and decompiling, produced accurate 3D models of the prosthetics. Shuxian et al. [6] described the limitations of the plaster-casting method in traditional prosthetic socket fabrication and emphasized the benefits of reconstructing the 3D models for bones and skin of the residual limb via two-dimensional CT scanning, using image processing and reverse engineering techniques. This process was shown to accurately reconstruct the 3-D model of both the internal and the external structure of the residual limb and facilitate customization of bespoke prosthetic socket design for individual patients. Both the studies [5] and [6] also confirmed the suitability of computer-based techniques for achieving excellent details of the stress interface and load distribution on the residual limb and testability with gait cycles for effective functional performance. These investigations have further shown that computational methodologies mitigate the need for any invasive procedures, making this a good choice for patients, and workers due to the time efficiency, since models can be continuously refined and accommodated to each patient as per their measurements. This validates the use of FEA stress analysis, as an effective and sustainable method of evaluating the design of a prosthetic, as the results can be directly transferred to an actual prosthetic, pending specific measurements. These studies [5, 6] also discussed the minimal need for medical testing. Rohjoni et al. [7] studied numerically the stress patterns in transtibial prosthetic during gait cycle based on a static finite element analysis in CATIA software. They produced digital mock-up (DMU) kinematic simulations and examined a series of assemblies for a wide variety of joint sizes. They further considered whether the prosthetic will be active or passive, as this has a significant impact on the design and can also add limitations to the study as a passive prosthetic will have significantly less range of movement (ROM). They studied Polylactic Acid (PLA), for the prosthetic which was 3D printed for commercial production benefits. The movement of the prototype design modelled was based on deviations of angle between pylon and foot which were detected by rotary angle sensor which then triggered the DC motor to operate. Static analysis showed that peak von Mises stress is located at the foot at toe off. The highest von Mises stress at the pylon beam was 995MPa with a stress of 156MPa on top of the pylon during heel strike. Furthermore, the foot demonstrated a peak stress up to 3.18MPa. Prochor and Sajewicz [8] deployed ANSYS software to study the optimal thread shape deployed in implants for direct skeletal attachment of limb prosthesis, motivated by reducing user comfort and pain in the remaining limb by modifying proper parameters obtain maximum efficiency. They used between 325,000 and 375,000 finite elements with maximal edge length of 3.0 mm for the implant-bone model. They showed that in the case of axial loading, the highest values of analysed stress peaks were generated at a flank angle of 25°. Similar dependencies were observed in the case of heel strike, but in this case, equivalent and longitudinal stress peaks were the highest with a flank angle of 45°. Additionally, as in the axial loading, the radial and transverse stress peaks were characterised by the highest value at a flank angle of 25°. The best stress peak reduction was obtained by modifying only the rounding arc increasing it by 0.2 mm, leaving the flank angle at a normalised value of 35°. Overclosure is the most popular way of modelling socket loading whereby the socket and residuum are considered a singular body; however, the prosthetic and limb are given different mechanical properties – see Winson et al. [9]. Overclosure is a simplified method that yields reliable results, hence its popularity. Donning is where the socket slides onto the limb to create a point of contact, and this creates a small step for stability, before fully locking the socket onto the limb. Steer et al. [10] developed a parametric finite element model in ABAQUS with contact mechanics using magnetic resonance imaging data from a person with transtibial amputation. They conducted comparative numerical stress analyses for different socket loading methods, socket–residuum interface parameters and soft tissue material models, to quantify their effect on the residuum's biomechanical response to a range of parameterised socket designs. They emphasized that the choice of modelling approaches (i.e. donning vs. overclosure) and selected input parameters (i.e. material properties) exerts critical influence on the predicted biomechanical response of the limb under prosthetic loading, and that less accurate interface models can result in inadequate clinical fit for the prosthesis user and, in extreme cases, development of skin and sub-dermal tissue damage from adverse pressure and shear gradients. Boudjemaa et al. [11] used stereolithography MIMICS 3-MATIC software and Autodesk Meshmixer to conduct 3-D stress simulations of stump–prosthetic interface mechanics to highlight the zones experiencing the highest levels of stresses. They customized the prosthetic socket and liner designs to precisely fit the unique contours of the residual limb with careful resolution of the contact surfaces to accommo¬date and smooth any cavities or irregularities. They observed that designed liner was highly effective in reducing stress, particularly in three critical areas: the lateral area of the tibia head (LTH), the tibia end area (TE), and the fibular end (FE). Stress values at the LTH were shown to decrease from 55 to 10 kPa, at the TE from 60 to 28 kPa, and at the FE from 72.3 to 14 kPa. Their study showed that the liner represents a bespoke intervention, and finite element modelling is an excellent predictive tool that not only identifies critical stress points but also guides the design of personalized prosthetic liners to enable improved wearer comfort and reduction of the risk of skin-related complications for persons with disabilities. Cherif et al. [12] applied Abaqus finite element stress simulations to determine how liner material (Gel vs. Silicone) and thickness affect contact pressure, maximum principal strain, shear stress and vertical displacement at the residual limb-liner interface. They showed that liner thickness plays a critical role in modulating pressure distribution and mechanical stability, with Gel providing superior flexibility and shock absorption, whereas Silicone offers enhanced structural integrity. They further noted that at a thickness of 2 mm, maximum pressure of 0.4656 MPa is recorded whereas with liner thickness of 4 mm, the pressure decreases to 0.4153 MPa, producing a stress reduction of approximately 10.8%. Further increasing the thickness to 6 mm was found to induce further pressure drop of 0.3825 MPa, corresponding to a total reduction of 17.9%. The simulations overall demonstrated an excellent strategy for achieving stress attenuation mechanisms, contributing to the optimization of prosthetic liner design for improved clinical outcomes in lower-limb amputees. Barattini et al. [13] reported on finite element structural dynamic and stress analysis of the carbon fibre-based Cheetah Xcel commercial lower limb prosthetic (for sports activities) manufactured by Össur. They also conducted experimental vibration tests. They utilized LUPOS 2023 (LUmped Parameter OpenSource FEM code developed in Matlab) and conducted real modal analysis in MSC Nastran 2017, using 3D hexagonal elements (CHEXA). They focused on investigating the dynamic behaviour of a running blade prosthetic and developing a validated prosthetic model, with careful definition of suitable material properties. They presented novel results for blade prosthetic dynamic characteristics in free–free conditions and measured the first six mode shapes in the frequency range up to 750 Hz, including both bending and torsion. They observed that the bending in the vertical plane constitutes the primary mode shape which elevates energy storage, enabling athletes to achieve an optimal running gait and emphasized that anisotropic properties can contribute to accuracy in finite element models.

The standards for prosthetics and orthotics are currently outlined by the World Health Organisation (WHO), as supported by the International Society for Prosthetics and Orthotists (ISPO). When discussing the products sector of such regulations set out by the WHO, it is important to understand what is meant by an 'appropriate product', according to the official guidelines, a product is appropriate, only when it fits the specific needs of the user, including a true fit and alignment to the user, and are economically feasible [4]. Cost-effectiveness is not a new issue, it is well known that prosthetics are an expensive solution to loss of limb, as opposed to stand-alone physical therapy (PT) and occupational therapy (OT), to help people adjust without any substitute or artificial limb. Conducting finite element simulations on lower limb prosthetics with different materials is an inexpensive and valid methodology for developing more cost-effective designs in practice. Basing models on existing commercial designs is important. In the current study we will examine the "Sara Diogo" prosthetic [14], visualized among other commercial designs in Fig. 1. This is a complete lower limb prosthetic unlike other designs which are focused on the foot. Össur [15] is also a leading manufacturer for prosthetic and orthotic devices, and have a range of lower limb devices, including sockets, knees, and feet. The Pro-Flex is a range of foot prosthetics, which covers a variety of needs and activity levels, following the same trademarked pattern. The Pro-Flex XC Torsion design is weatherproof and anatomically similar to a standard foot, which is important for both aesthetic purposes, for example shoe options, but also for comfort and user ease. The foot contains a vertical shock pylon for improved shock absorption, as well as rotation and movement in line with the natural tibial movement that would be seen when walking with a full leg. Another design produced by the Steeper Group is the Freedom DynAdapt, which is a carbon fibre, water resistant foot, that is also designed for high impact [16]. The design allows users to move more freely across uneven terrain than other market leaders. Additionally, it is made from an advanced composite laminate (carbon fibre). The benefits of this include the high cycle fatigue, providing durability to the foot, and security that it will last to the user. The material returns high energy too which assists in the mobility of the prosthetic device. Finally, Ottoblock produce a variety of mobility aids, as well as orthotics and prosthetics and among their products is the Maverick Comfort AT prosthetic foot [17], which uses fibre glass for durability. Fibre glass is resistant to abrasive waters such as salt and chlorinated water. It has a comparable weight limit to the Freedom DynAdapt from the Steeper group, despite the different composite material. Composites are the popular choice as they are lightweight, yet durable. Again, as with the DynAdapt, it has a high energy return due to the lay-up of the lamina in the material.

Another main issue with prosthetics, and often the primary factor in amputees declining a prosthetic device is the degree and type of pain which may be experienced during normal walking or stumbling, tripping etc [18]. The pain complaints of users of prostheses are both connected to the joint/residual limb, and the skin around where the prosthetic attaches to the user. Some of this pain can be felt due to gate deviation caused by the prosthetic and finite element studies may assist in identifying where there are areas of higher stress, so that design adjustments can be executed to minimize stresses and aid in returning the gait to its normal. Pressure in another key aspect that impacts the functionality and user comfort with prosthetics. The larger the surface area the pressure is distributed over, the lesser the point load on the residuum, hence a more comfortable function. A relative proportion of residuum areas can withstand enough pressure to function normally, without many adjustments to the socket/prosthetic. However, there are still a number of prosthetic users who are sensitive to the forces applied on the residuum, particularly the pressure, therefore it is a general recommendation to still ensure that the pressure exerted is distributed evenly over the largest possible surface area, subsequently reducing the point load and increasing comfort. Although this specifically helps those who are sensitive to the pressure, a lower point load is still going to increase user comfort for majority of the amputees, as well as reducing point sores and irritation to the residuum from the socket. Comfort and functionality can be viewed as a correlation, the more comfort the user experiences, the more inclined they are to use the prosthetic and follow through rehabilitation, henceforth the function of the remaining limb and their body will increase, as the kinetics return more towards typical body kinetics of none-amputees. An additional key aspect of prosthetics is the suspension system chosen; the suspension system is the section of the prosthetic that keeps the device attached to the residuum. The suspension supports two key forces, these are rotation, and shear. In addition to this, a good suspension system is key to comfort and proprioception. Proprioception is the ability the body has to recognise its parts, and how they feel/move. The support with proprioception also increases control as the body has a greater ability to sense itself, in this case it would be sensing the residuum and the forces upon it, in order to move and use the prosthetic more efficiently. Efficiency is important for conservation of energy, the less energy needed to move, due to less force needing to be exerted to use the limb, can lead to comfort and use for a prolonged period of time. Rotation is important to consider for ergonomics and comfort. When discussing suspension systems, rotation primarily applies to the rotation of the residuum within the system, this is contrary to the rotation of the foot/ankle which is relevant when discussing the moment of resistance. Shear and normal forces both act on the residuum and prosthetic. Shear is the more important of the two forces to consider when discussing suspension. When discussing prosthetics, the shear force is seen on the limb moving backwards and forwards as with normal walking movement, and the skin on the residuum also pulling upwards. Primary examples of suspension within a prosthetic are suction, belts and straps, sealing liners, and self-suspending, also known as supracondylar suspension. Having a strong and suitable suspension system is paramount to an amputee, as their bodies rely on this for good proprioception, being able to sense the whole of the prosthetic limb from the residuum. The choice of suspension system can depend on a number of factors, such as cosmetics, length and stability of the residual limb, joint stability, and vascular supply [19]. There are other factors that can be difficult to predict, such as changes to the volume in the leg, often due to oedema from overuse or adjusting to the prosthetic.

In the current article, we describe recent finite element stress analysis simulations using ANSYS APDL/WORKBENCH is conducted for a robust geometry resembling a lower limb prosthetic inspired by the "Sara Diogo" design [14]. A parametric study of different loading conditions is conducted to both evaluate the suitability based on the current available prosthetics, and to critically evaluate the results against pre-existing studies to check validity. Carbon fibre, Epoxy Carbon Woven Prepreg and E-Glass are the 3 selected composite materials based on a careful study of current materials deployed in prosthetics design. SOLIDWORKS is deployed to create a 3-D prosthetic geometry. Appropriate loading conditions are imposed. Static stress analysis simulations are conducted for different materials. Mesh independence tests are also conducted. Equivalent elastic (Von Mises) stress, equivalent strain, maximum principal stress and total deformation plots are presented for all three composite materials examined. The present simulations may be beneficial to prosthetic designers in particular with regard to cost-effectiveness and material specifications with regard to longevity.


**Fig 1:** ***From left- Sara Diogo" prosthetic, next Össur Pro-Flex XC Torsion foot, next Steeper group DynAdapt, finally Ottoblock Maverick Comfort foot design- reproduced with permission.***

## 2. SolidWorks Geometric Modelling

As aforementioned, the FEA within this study has been conducted using ANSYS, more specifically ANSYS Workbench 2022 R2. In order to construct and format the model, Solidworks 2023 and GrabCAD were also used. The prosthetic model used was adapted from the Sara Digo geometry [14]. It was designed using Solidworks, making it compatible for the software she was chosen for this study. Additionally, the files were in ".step format". The 3-D lower limb prosthetic geometry was loaded into Solidworks. Fig. 2 shows the different elevations of the Solidworks model. Appropriate dimensions are extracted from [14]. The geometry must be first constructed in Solidworks in order to export the file in the correct, readable format into ANSYS APDL/workbench and the file is therefore exported as .wbpj file. It is important to note that prosthetic designs are continuously evolving commercially. However, the essential features are captured in Fig. 2 including the support, ankle, suspension etc and the model adopted does follow the general skeleton design utilized in most company examples.

## 3. ANSYS Finite Element Simulations

### *3.1. Analysis type*

ANSYS workbench 2022 R2 software is deployed for the finite element steady static linear stress analysis of the Solidworks model. The ANSYS software is extremely versatile. It has been successfully deployed by the authors in an extensive range of mechanical, biomedical and aerospace engineering stress analysis and also fluid-structure interaction (FSI) problems including ocean engineering membrane wave converters [20], thermal stress analysis of clay-barrier geological nuclear waste storage facilities [21], aircraft seat structural dynamics [22], honeybee inspired micro air vehicle wing structural analysis [23], high temperature corrosion- resistant coatings for aircraft turbo engine blades [24], fluid-structure interaction in composite aircraft wing delamination from water penetration [25], peristaltic pumps for chemical wastes [26]. All matrix formulations intrinsic to ANSYS stress analysis are given in the Appendix. With prosthetics, there is usually a singular load bearing on the limb, the specific point of this load is dependent on the design of the limb. In the case of the present limb design used we assume a singular point on the top of the limb, where the load is applied. As such the force is also steady and does not simulate the different variation in force encountered when walking i.e. the dynamic distribution of forces in the gait cycle. The present simulation however provides a solid base for future extension to consider dynamic gait forces.

### *3.2. Material Data*

Selecting the engineering data is the next step that must be taken in order to define the materials and their properties. For the prosthetic, we study carbon-based composite materials which due to high strength and low density are deployed in the vast majority of modern prosthetics. The materials initially chosen were carbon fibre, epoxy carbon woven prepreg, and e-glass. The data is extracted from the ANSYS materials database and other sources. ANSYS defaults to structural steel, and this is the material that is used when conducting the mesh convergence study. It is however modified for further simulations with the appropriate composite material properties. Figs. 3-5 show the material engineering data for all three composites deployed. It is noteworthy that in prosthetics, carbon fiber composite material properties depend heavily on the fiber type and orientation.

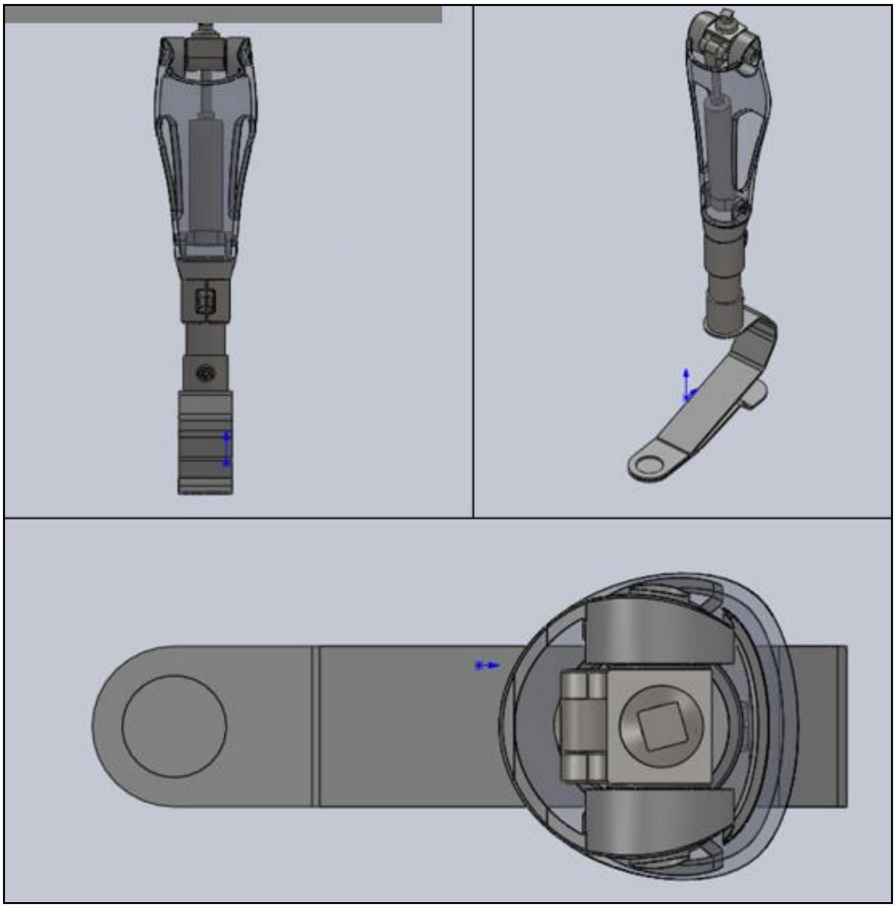

**Fig 1: Top left- rear view of SolidWorks design, top right- isometric view, below plan elevation.**

Carbon Fiber (395 GPa)

Fibers only

| | | |
|---|---|---|
| Density | 1800 | $kg/m^3$ |
| **Structural** | | |
| Orthotropic Elasticity | | |
| Young's Modulus X direction | 3.95e+11 | Pa |
| Young's Modulus Y direction | 6e+09 | Pa |
| Young's Modulus Z direction | 6e+09 | Pa |
| Poisson's Ratio XY | 0.2 | |
| Poisson's Ratio YZ | 0.4 | |
| Poisson's Ratio XZ | 0.2 | |
| Shear Modulus XY | 8e+09 | Pa |
| Shear Modulus YZ | 2.1429e+09 | Pa |
| Shear Modulus XZ | 8e+09 | Pa |

**Fig 2: Material properties of carbon fibre**

Epoxy Carbon Woven (395 GPa) Pre...

| | |
|---|---|
| Density | 1480 kg/m³ |
| **Structural** | |
| Orthotropic Elasticity | |
| Young's Modulus X direction | 9.182e+10 Pa |
| Young's Modulus Y direction | 9.182e+10 Pa |
| Young's Modulus Z direction | 9e+09 Pa |
| Poisson's Ratio XY | 0.05 |
| Poisson's Ratio YZ | 0.3 |
| Poisson's Ratio XZ | 0.3 |
| Shear Modulus XY | 3.6e+09 Pa |
| Shear Modulus YZ | 3e+09 Pa |
| Shear Modulus XZ | 3e+09 Pa |

**Fig 4: Material properties of epoxy carbon woven**

E-Glass

Fibers only

| | |
|---|---|
| Density | 2600 kg/m³ |
| **Structural** | |
| Isotropic Elasticity | |
| Derive from | Young's Modulus and Poisson's Ratio |
| Young's Modulus | 7.3e+10 Pa |
| Poisson's Ratio | 0.22 |
| Bulk Modulus | 4.3452e+10 Pa |
| Shear Modulus | 2.9918e+10 Pa |
| Isotropic Secant Coefficient of Thermal Expansion | 5e-06 1/°C |

**Fig 5: Material properties of E-glass**

### *3.3. ANSYS meshing*

The next step in pre-processing is importing the geometry. This is done by editing the geometry in "Design Modeler". This enables the user to import an existing geometry in file format that is readable by ANSYS, including the individual components, which is relevant for selecting the materials and applying the forces. Fig. **6** shows the imported geometry in ANSYS Workbench. From here each component can be selected individually, alternatively, all of the components can be selected together to define the material, prior to running the simulation. As this is a simplified simulation, the same material is applied for each of the three simulations to the whole model.

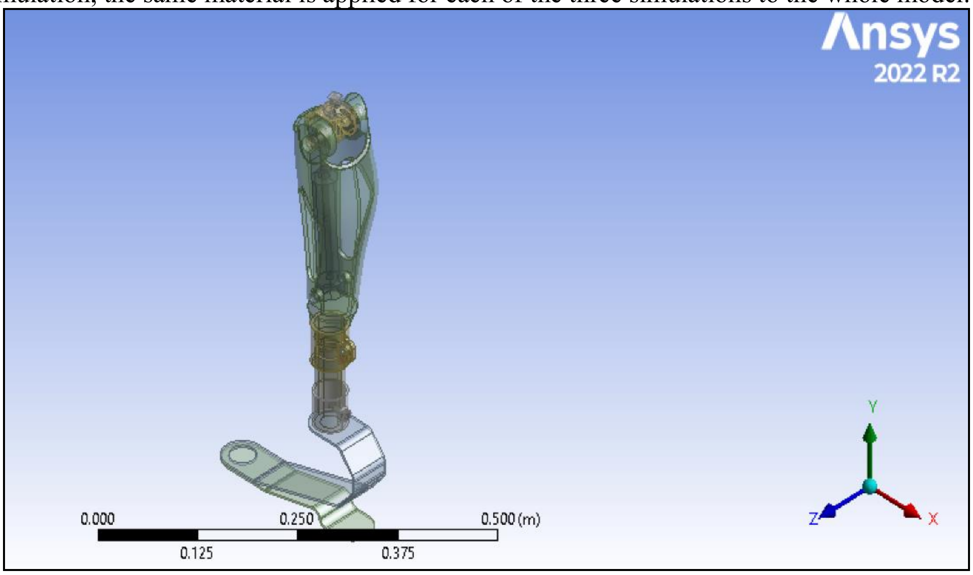


**Fig 6: Imported prosthetic geometry in Workbench 2022 R2**

*3.4. Boundary conditions - forces and fixed points*

The final step of pre-processing is applying the forces and fixed points. As aforementioned, there is one static load applied to the top of the prosthetic in the -Y direction, to represent body weight, and is depicted in Fig. 7. This is a load of 600N which corresponds to the mass for an average person [27] on a global scale of around 62kg.

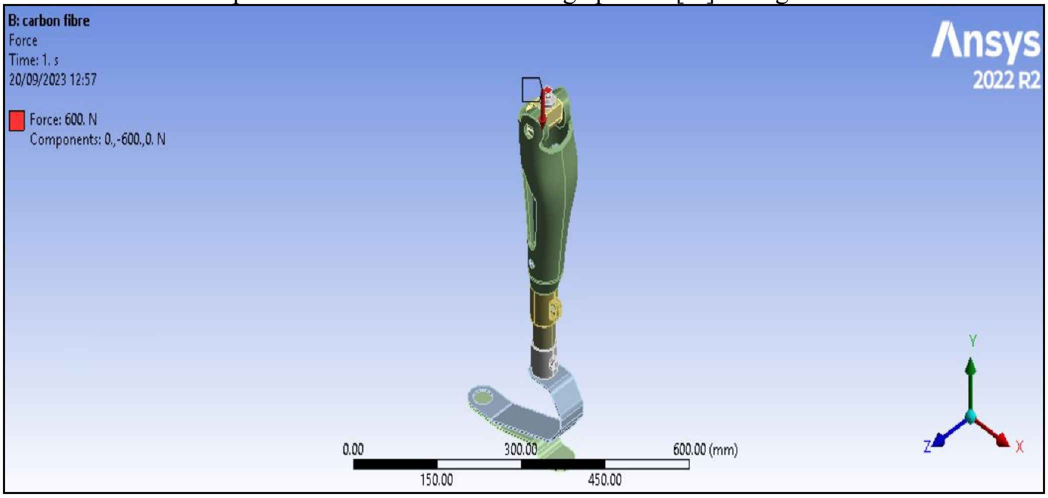


**Fig 7: Applied forces on body in Workbench 2022 R2**

| Details of "Force" | |
|---|---|
| Scoping Method | Geometry Selection |
| Geometry | 1 Face |
| **Definition** | |
| Type | Force |
| Define By | Components |
| Applied By | Surface Effect |
| Coordinate System | Global Coordinate System |
| X Component | 0. N (ramped) |
| Y Component | -600. N (ramped) |
| Z Component | 0. N (ramped) |
| Suppressed | No |

**Fig 8: Applied forces on body from menu**

The next force to be applied is gravity which is prescribed as 9.8m/s$^2$ (**Fig. 9**).

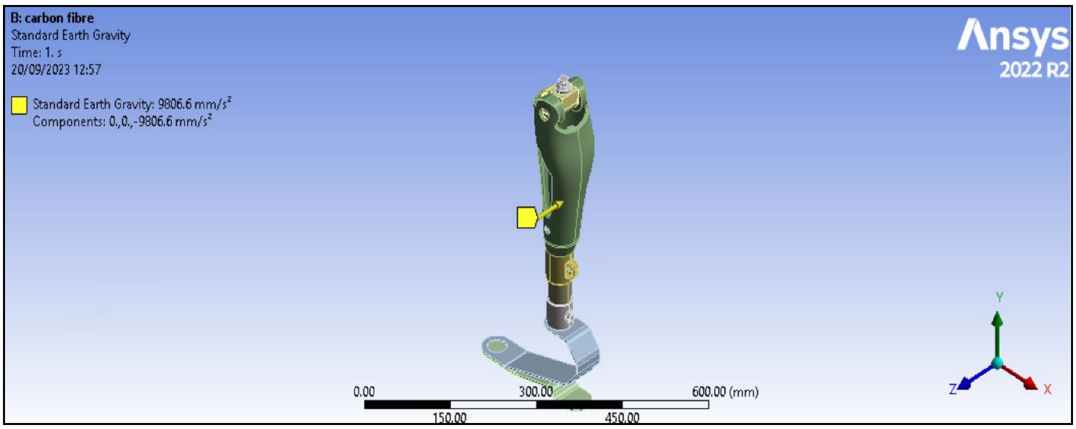


**Fig 9: Gravity applied on the prosthetic body**

The reason an average mass for a person was not taken from a specific country is as prosthetics are used globally, and for a wide demographic, therefore the most widespread average is the most suitable for the model. It is important to define correctly the direction and magnitude of the force. The force is also ramped, as seen in Figure 8, and has a defined magnitude and duration, in a set direction. Ramped forces in prosthetics describe the gradual, controlled build-up and distribution of weight-bearing loads (ground reaction forces i.e. GRFs) to prevent painful socket pressure and joint damage. This is particularly critical when traversing inclines, where adaptable prosthetic ankles automatically adjust their angle (dorsiflexion/plantarflexion) to smooth out GRF spikes [28].

The final stage of forces is to apply constraints to the model i.e. fixing components within Workbench. It is paramount to fix some elements within the model in order to obtain a more accurate result. The constraints within this model were applied to the heel and the ball of 'foot', these can be seen in Figure 10. These areas were chosen due to the movement on a leg when at rest. When stood on a foot, those are the aspects that are stationary as they rest on the ground, they are also the elements that bear the most force/mass. Additionally, not applying constraints to the model can flag up issues within the software surrounding the solutions.

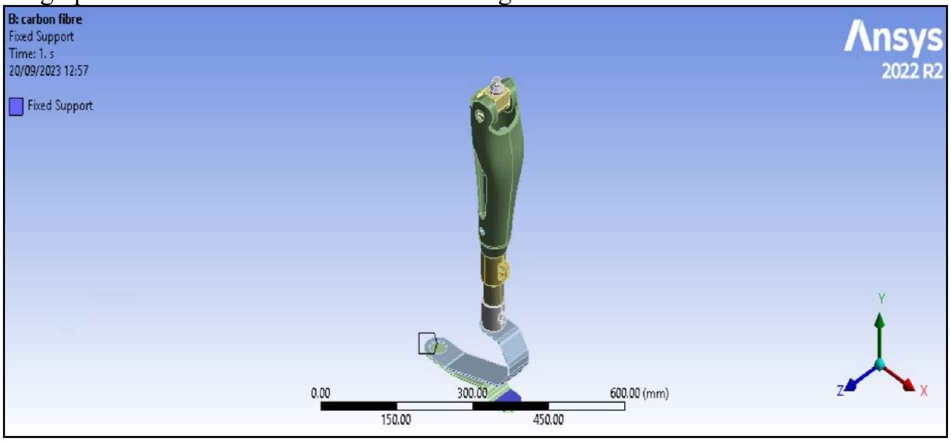


**Fig 10: Fixed supports on the prosthetic model**

### *3.5. Mesh independence study*

Meshing is the next key stage of the set-up for this analysis. Within Workbench, after loading the model, there is the option to mesh the prosthetic geometric model. A mesh convergence study is conducted in order to establish an appropriate range of sizes for the element length., and from this a single element length size is established and applied to each composite material case. We select the total deformation as the parameter to be checked. 3-Dimensional tetrahedral elements (pyramids) are deployed to accommodate the complex geometry. When mesh density is progressively increased, the residual is decreased and as convergence is approached the total deformation eventually begins to plateau. When insignificant variation is computed with two progressive mesh densities, the number of lowest number of elements at this point is acceptable for accuracy. The plateau is seen by plotting a graph of the total number of elements against the maximum deformation in mm. Multiple convergence studies with a number of mesh designs were conducted. It is noteworthy that with very fine meshing, excessive computational compilation times can result, and storage memory can be an issue. Refining the whole mesh can be a reason for inconsistency. It is common to locally refine the mesh at a specific area of interest, which often is the prosthetic foot area, since this invariably is the most impacted by the force, as the weight in a normal human foot is generally distributed between the heel and ball of the foot. However, in this study the whole mesh was refined, this does link with the previously mentioned point of storage and the mesh being too fine as it is a particularly large area to mesh. The reason that the decision was ultimately made to mesh the whole leg is as the forces are still distributed across the whole body. Table 6 shows the element dimensions, numbers of elements (mesh density) and associated total deformation computed in ANSYS. 7 different mesh designs were appraised. The element length is initially prescribed as 55mm. This size was chosen after some experimental measurements, and also from establishing the default number of elements that Workbench creates with the default mesh. The maximum deformation in the successful convergence study began to plateau at approximately 11,100 elements. Hence the element length chosen for all subsequent simulations was 45mm, as this is the lowest number of elements that achieves convergence. Fig. 12 shows the mesh convergence study results, and the plateau is clearly visible around 11, 100 elements confirming that the results are independent of the designed mesh density. In addition, we have visualized the meshing for all 7 prosthetic mesh density cases (based on the finite element dimension) in Figs. 13-19.

**Table 1: Mesh independence (convergence) study**

| Mesh design case | Element Length (mm) | No. of elements | Max. Deformation (mm) |
|---|---|---|---|
| 1 | 55 | 10679 | 20.213 |
| 2 | 53 | 10925 | 20.221 |
| 3 | 50 | 11035 | 20.578 |
| 4 | 47 | 11043 | 20.578 |
| 5 (selected) | 45 | 11097 | 20.953 |
| 6 | 43 | 11208 | 20.953 |
| 7 | 40 | 11346 | 20.953 |

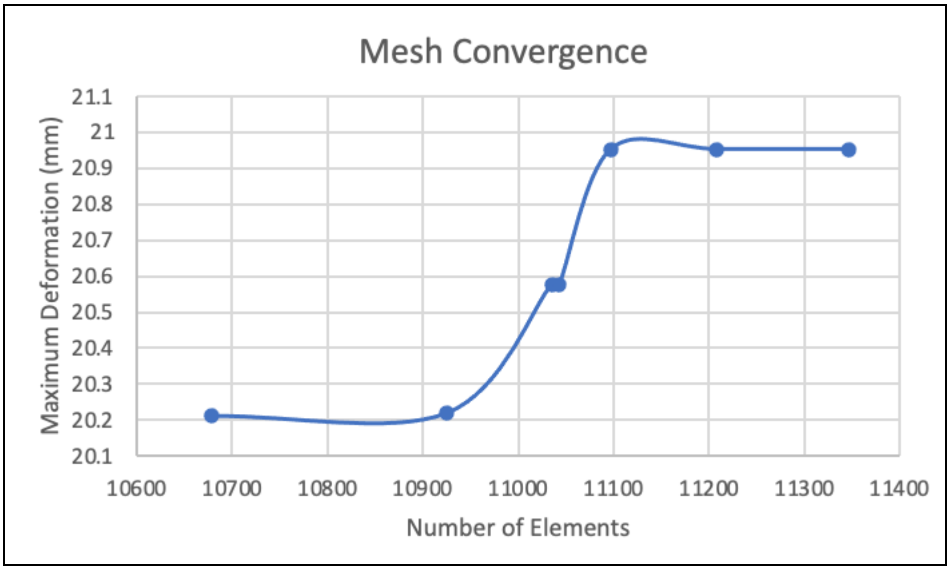


**Fig 12: Graph of mesh convergence study**

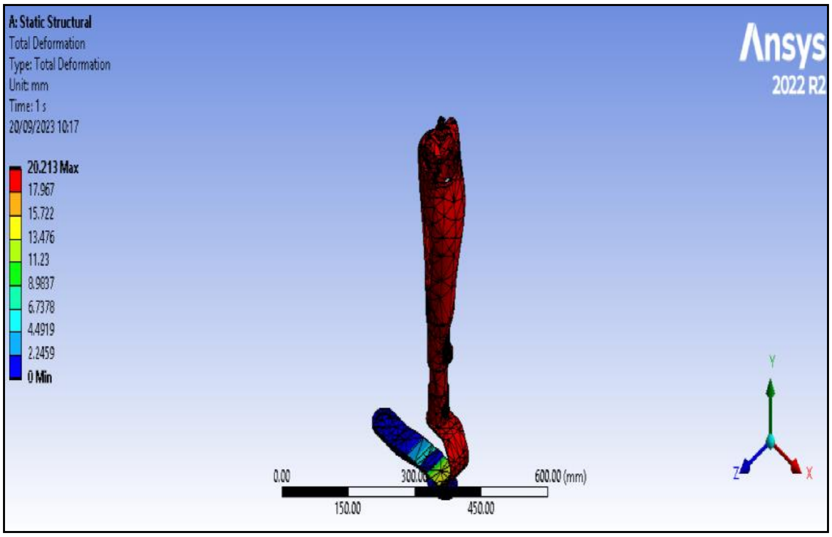


**Fig 13: Total deformation for mesh 1 with element length of 55mm**

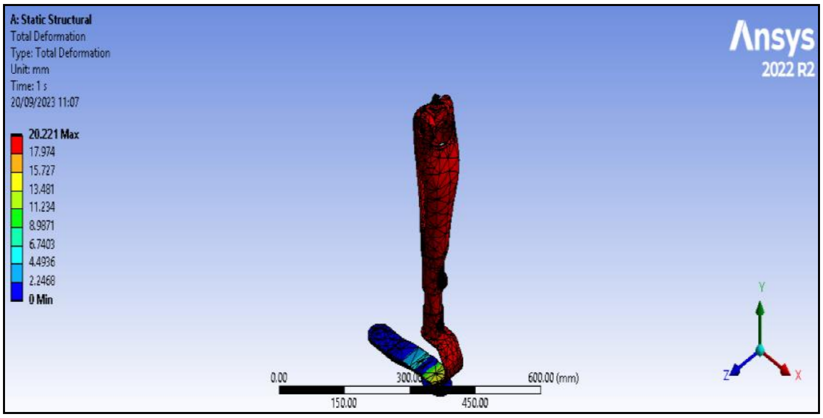


**Fig 14: Total deformation for mesh 2 with element length of 53mm**

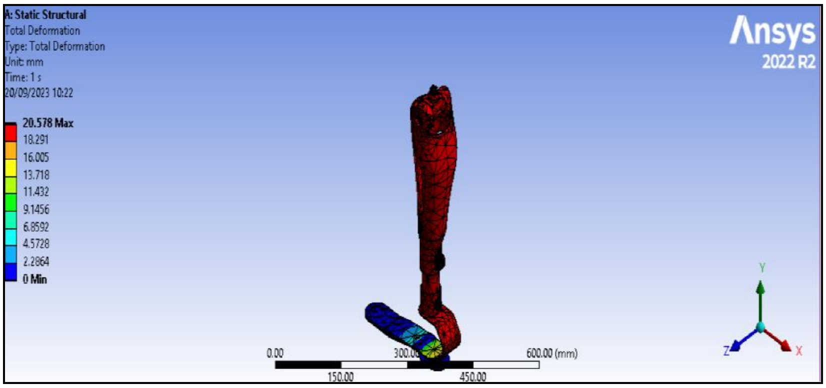


**Fig 15: Total deformation for mesh 3 with element length of 50mm**

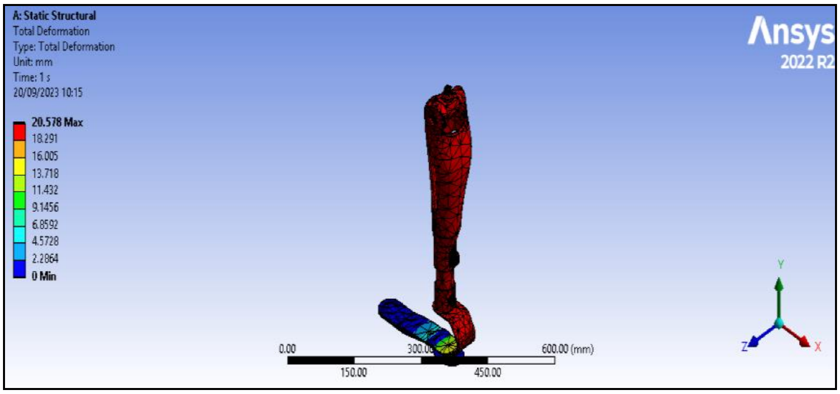


**Fig 16: Total deformation for mesh 4 with element length of 47mm**

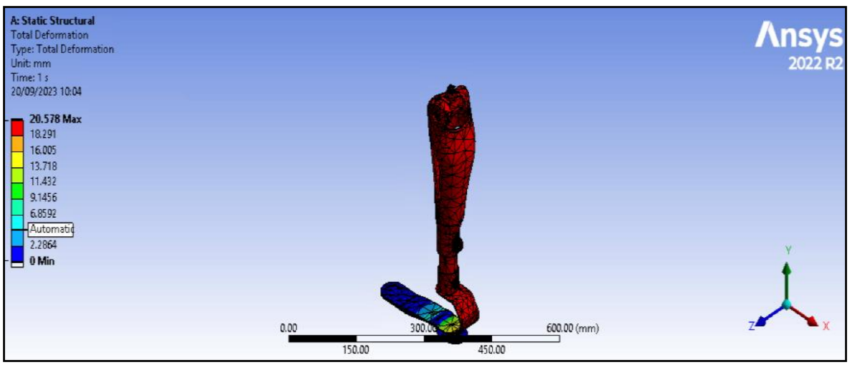


**Fig 17: Total deformation for mesh 5 with element length 45mm (converged)**

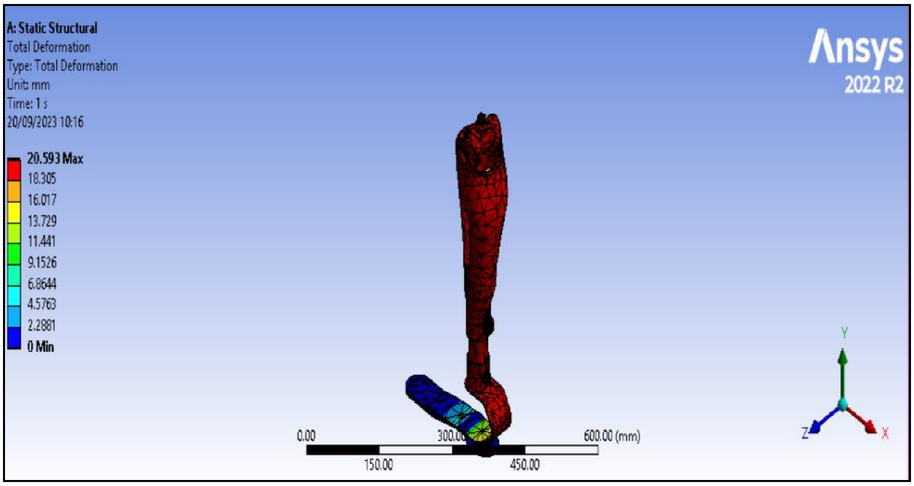


**Fig 18: Total deformation for mesh 6 with element length of 43mm**

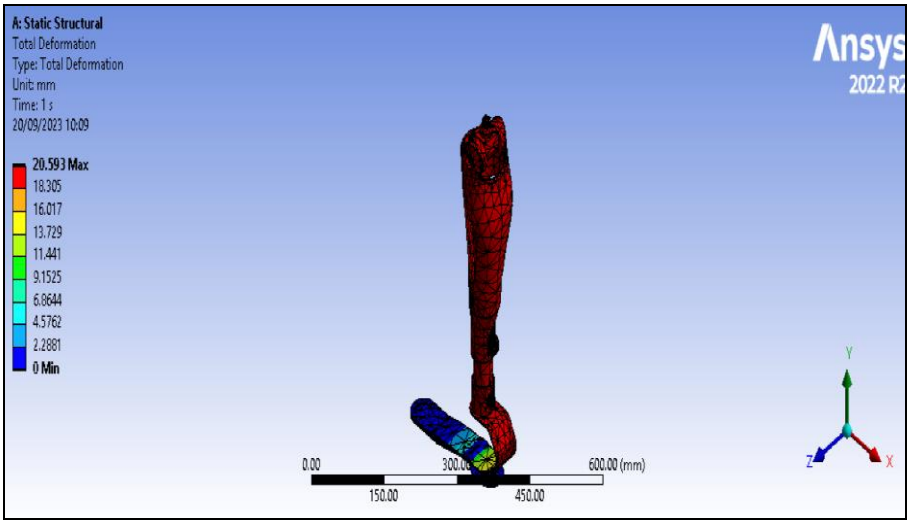


**Fig 19: Total deformation for mesh 7 with element length of 40mm**

## 4. ANSYS Results and Discussion

### *4.1. Total Deformation*

Figs. 20-22 visualize the total deformation contour plots for all 3 composite materials investigated. Table 2 gives the maximum total deformation computed for all 3 cases. Since material 3 i.e. E-glass is inherently a stiffer material, it is expected that this has the lowest deformation. The carbon fibre has one of the higher Young's modulus values. Furthermore, the epoxy carbon woven has the highest Poisson ratio, and lowest Young's modulus and shear modulus and it is expected that the deformation here would be the highest. The deformation in the carbon fibre and E-glass can be acceptable, however the deformation seen in the epoxy woven carbon is significantly high, at close to 15cm. This would provide considerable movement within the prosthetic and suggest the material is more relaxed than initially estimated. Therefore, epoxy woven carbon would not be sufficiently structurally should the entirety of the prosthetic be comprised of this. In addition, this could also cause significant instability and subsequent loss of balance for the user. These are obviously unfavourable qualities for a prosthetic as the point is to improve function of the residual limb and provide the user with stability, as well as attempting to return a normal gait to improve the quality of life. In general, the results seen are reasonable. In all cases minimal deformation is computed at the toe region (blue) with slightly greater magnitudes around the heel and ball foot zones. (green and blue zones). The maximum deformations (dark red zones) are always computed in the main vertical component of the prosthetic due to load transfer being significant here.

**Table 2: Extracted total deformation values compared for all three composite material prosthetic designs**

| Material | Total Deformation (mm) |
|---|---|
| Carbon fibre | 82.776 |
| Epoxy Carbon Woven | 146.15 |
| E-Glass | 58.064 |

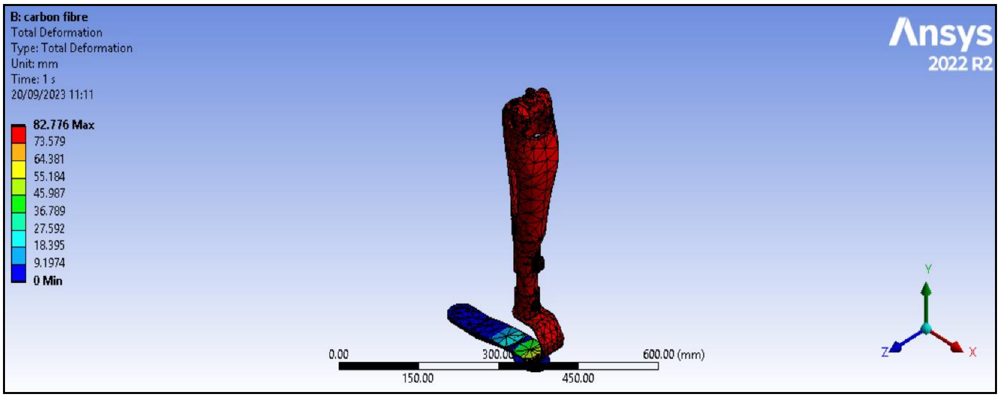


**Fig 20: Material 1: Carbon fibre total deformation**

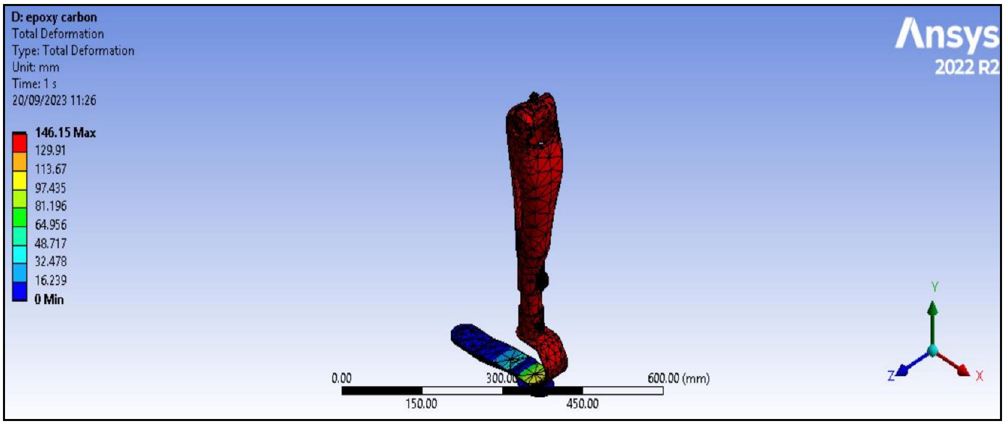


**Fig 21: Material 2: Epoxy carbon woven total deformation**

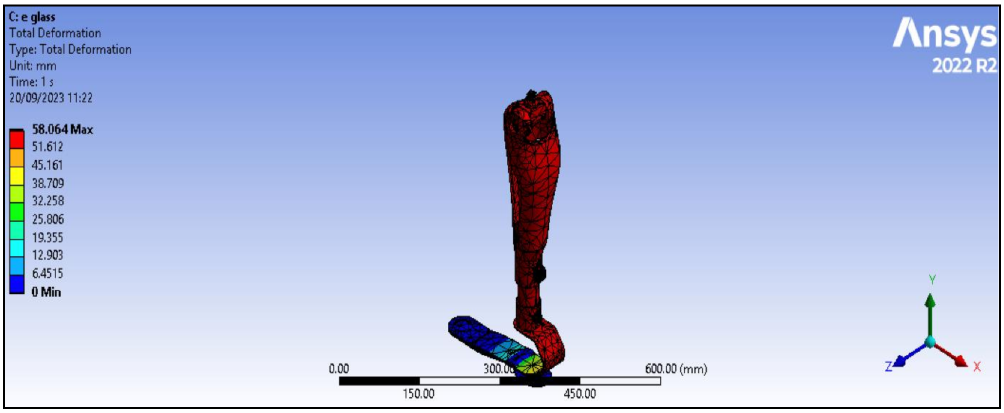


**Fig 3: Material 3: E-glass total deformation**

The three key properties varied for the 3 composite materials are: Young's modulus, Poisson ratio and the shear modulus (St Venant's modulus). Young's modulus is defined as the ratio of tensile stress (σ) to tensile strain (ε) [29]. The amount of force applied per unit area is the stress, and extension per unit length is the strain. Young's modulus can aid in establishing the stiffness of a material, how much it can stretch and deform. Each material will also have a limit of elastic deformation, before reaching plastic deformation (not returning to the original state). Young's modulus of the composite material therefore plays a critical role in establishing which material experiences the highest deformation, and this is intimately related to the prosthetic patient comfort. It also indicates which material is the most prone to plastic deformation and therefore will suffer from a shorter lifespan for materials with a lower Young's modulus. As prosthetic legs are constructed with the idea of longevity, it is not only financially beneficial, but beneficial to the user, to ensure that the material can safely deform elastically for a prolonged period of time. Carbon fibre and epoxy woven carbon have the highest Young's modulus. This makes them significantly more suitable than E-glass for a prosthetic leg as they will not deform as much under the forces applied. However, there are different benefits to a lower Young's modulus, for example comfort for the user as there is more space for deformation. Nevertheless, this can also be a negative, as too much deformation can cause plastic deformation, since too much movement under the forces applied can bring stability into question and whether the user of the prosthetics' gait would be affected by the potential lack of support due to this additional movement. Poisson's ratio is another fundamental structural material property that quantifies how much a material expands in perpendicular directions when compressed or thins when stretched. Mathematically, it is the negative ratio of transverse (lateral) strain to axial (longitudinal) strain [23, 27]. Ideally, a low Poisson ratio is desired when identifying a material that does not deform easily. Composite materials with a high Young's modulus, will have a lower Poisson ratio. The lowest Poisson ratio corresponds to epoxy carbon woven pre-preg. However, all of the materials present a similar and relatively low Poisson ratio which in theory should control maximum deformations sustained in the prosthetic. The consistently low Poisson's ratio supports the choices for these materials, as it suggests they all share structural properties which make them fit for purpose in prosthetic applications. Finally, shear modulus is the ratio of shear strain to shear stress. It quantifies the material's resistance to elastic deformation when subjected to a force parallel to its surface (shear stress). It is desirable (as with Young's modulus) for a material to have a higher shear modulus, as this indicates it is more resistant to shear deformation. Shear deformation is different to other deformation, since the material does not change in length/height, but still undergoes deformation (e.g. it may stretch slightly horizontally). E-glass presents the highest shear modulus, since it is a glass-based composite. Overall, all three composite materials however fall within comparable values for the shear modulus.

### *4.2. Equivalent Elastic Strain*

Figs. 24-26 depict the maximum equivalent strain for all 3 materials examined. This refers to the point of the material that undergoes the most strain and is the most prone to failure [22, 23, 27]. Stress is used in conjunction with strain in order to establish the yield strength of a material. In addition, elastic strain can aid in the prediction of the ultimate strength of a material. In ANSYS equivalent elastic strain is a scalar value calculated from the six individual strain tensor components using the von Mises yield criterion. It condenses complex multi-axial states of strain into a single positive value, typically used to evaluate if a material's distortion indicates potential yielding or fatigue life. A higher elastic strain result can suggest that the material can undergo more strain before permanent plastic deformation, as discussed when defining the material properties. Table 3 gives the maximum equivalent elastic strains for all 3 cases. E-glass has the lowest elastic strain, and epoxy carbon woven has the highest elastic strain. Again, these results fit the expected values, with similar rations of elastic strain to deformation. A material with higher stiffness, such as E-glass (Fig. 26), will have less elastic strain, as it will undergo plastic deformation much sooner than that of a material with more deformation. Carbon fibre remains the most suitable choice for prosthetics as it provides some elasticity, without compromising the shape of the design, and additionally allowing room for movement, increasing user comfort (Fig. 24). Epoxy carbon woven equivalent elastic strains (Fig. 25) are much higher than the other two materials again indicating undesirable performance for prosthetics.

**Table 3: Extracted equivalent elastic strain values compared for all three composite material prosthetic designs**

| Material | Equivalent Elastic Strain (von-Mises) |
|---|---|
| Carbon fibre | 0.034523 |
| Epoxy Carbon Woven | 0.065127 |
| E-Glass | 0.011818 |

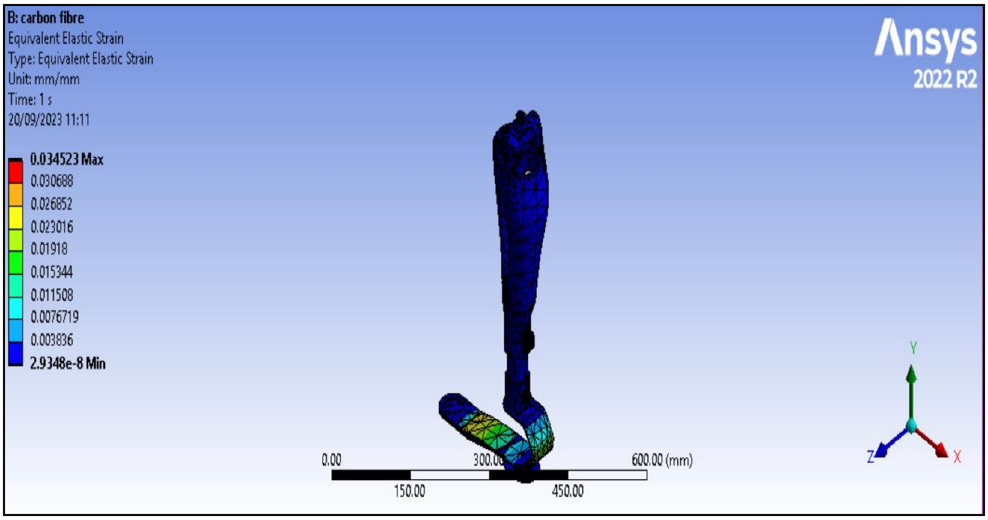


**Fig 24: Material 1: Carbon fibre equivalent elastic strain**

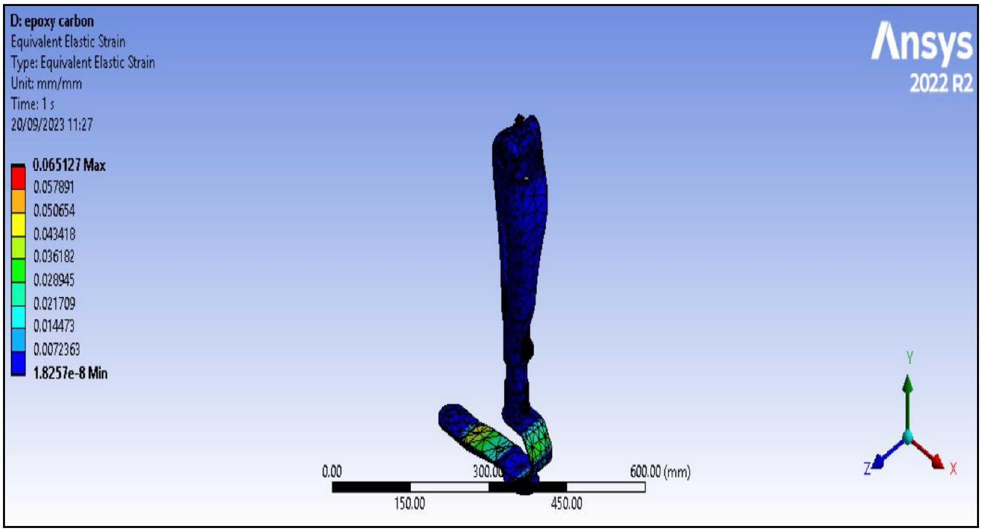


**Fig 25: Material 2: Epoxy carbon woven equivalent elastic strain**

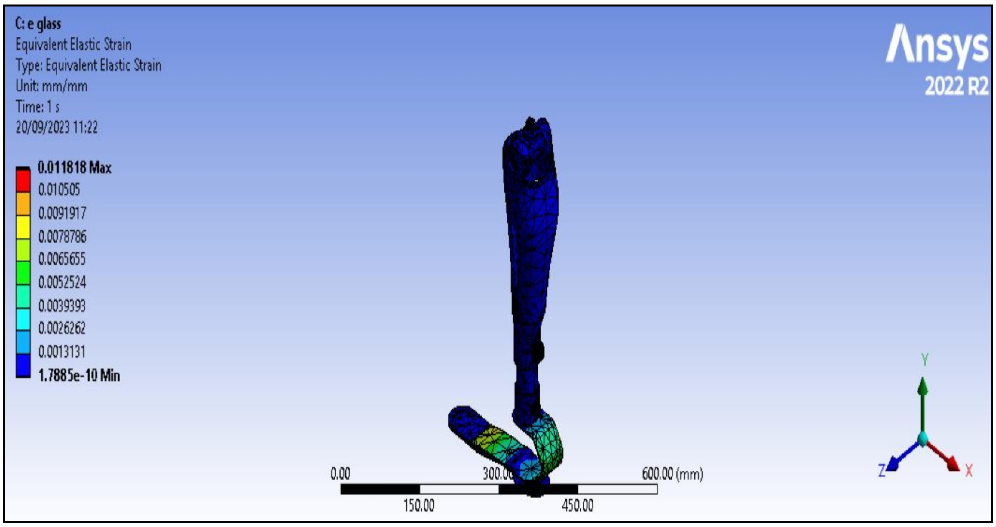


**Fig 26: Material 3: E-glass equivalent elastic strain**

### *4.3. Equivalent Stress*

Figs. 27-30 display the equivalent (Von Mises) elastic stress for all 3 composite prosthetic simulation cases. Table 4 gives the maximum equivalent elastic stress for all 3 cases. The equivalent stress in ANSYS refers to the von Mises stress, which condenses complex 3D stress states (tensor data) into a single scalar value. It is primarily used to determine if a ductile material has yielded or reached its failure point. ANSYS defaults to showing averaged nodal stresses, which smooths out contours between elements. As well as the equivalent stress, the principal stresses can also be calculated (described in sub-section 4.4). The material will not yield, as long as the von-Mises stress does not exceed the yield strength of the material. Carbon fibre is a unique example of a material as it essentially has no yield strength, this is due to the fact that it does not deform below the usual ultimate tensile strength of the material [27]. Therefore, whilst it has the highest von-Mises stress, it also will not be higher than the yield strength, as generally this upper limit does not exist. This could also be said for all composites, as they do not typically have a yield strength, the von-Mises stress will also be high. It is also possible to see plastic and elastic deformation co-existing in a composite, as the stronger/more solid parts of the composite will deform long after the 'softer' material holding them together. Carbon fiber (CF) woven with epoxy offers superior stiffness, lighter weight, and higher tensile strength compared to E-glass and epoxy composites. It is ideal for applications where every gram matters and flexing needs to be minimized. Carbon fiber is significantly stiffer (up to 3–5 times stiffer) and lighter than E-glass, allowing prosthetic biomechanical engineers the latitude to create thinner, unyielding components. However, E-glass is much more flexible and resilient to hard impacts. Carbon fiber is more brittle and can shatter or crack under high point loads.

**Table 4: Extracted Von Mises (equivalent elastic stress) values compared for all three composite material prosthetic designs**

| Material | Equivalent Stress (von-Mises) (MPa) |
|---|---|
| Carbon fibre | 1400 |
| Epoxy Carbon Woven | 925.07 |
| E-Glass | 816.65 |

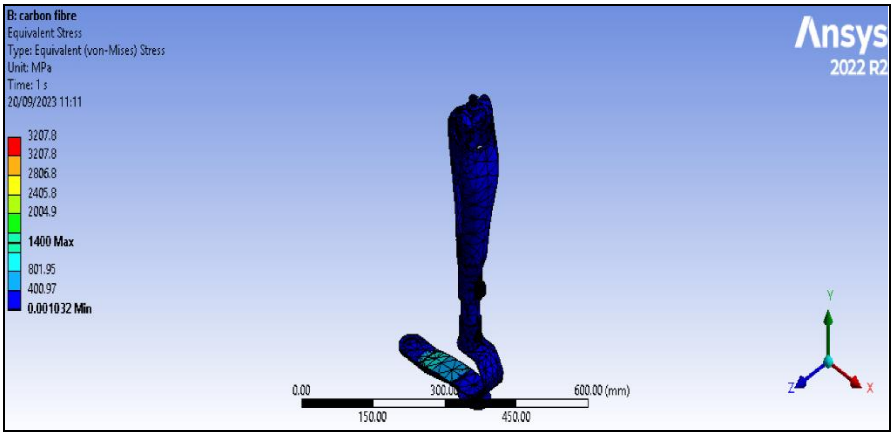


**Fig 27: Material 1: Carbon fibre von-Mises stress**

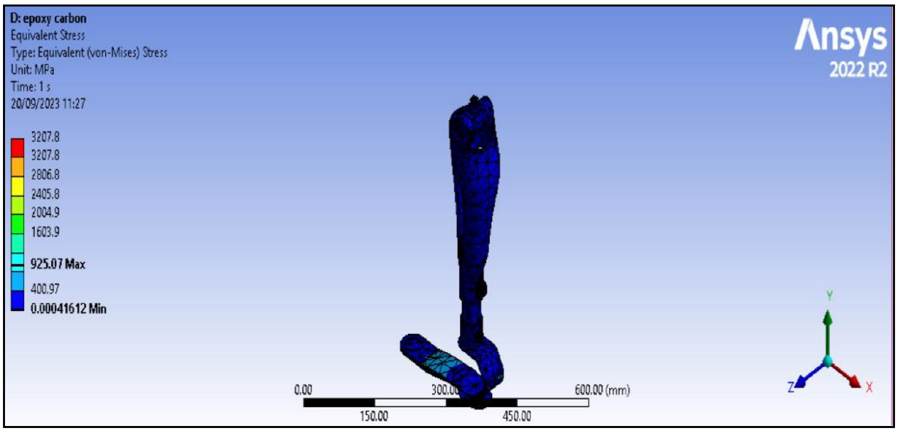


**Fig 28: Material 2: Epoxy carbon woven von-Mises stress**

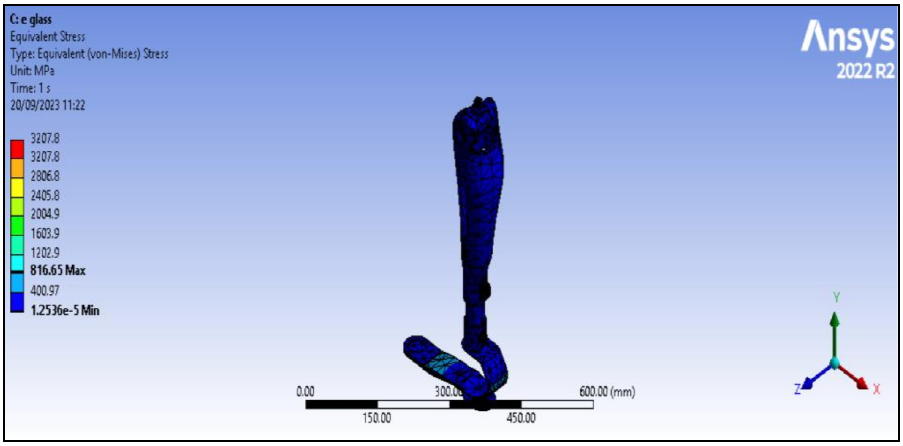


**Fig 29: Material 3: E-glass von-Mises stress**

### *4.4. Maximum Principal Stress*

The maximum principal stress contour plots, as shown in Figs. 30 to 32 have also been included as this is an industry standard intrinsic to prosthetics testing for different materials. This is 'normal stress" and can be useful to help visualize the stress patterns for the different composites. Table 5 gives the maximum principal stress values obtained via ANSYS for all 3 cases. As expected, the values for maximum principal stress align quite closely with the von-Mises stress results of Table 4. Much lower principal stress is computed for E-glass relative to Epoxy Carbon Woven composite and the latter is also significantly lower than for carbon fibre.

**Table 5: Extracted maximum principal stress values compared for all three composite material prosthetic designs**

| Material | Maximum Principal Stress (MPa) |
|---|---|
| Carbon fibre | 1397.8 |
| Epoxy Carbon Woven | 934.37 |
| E-Glass | 808.19 |

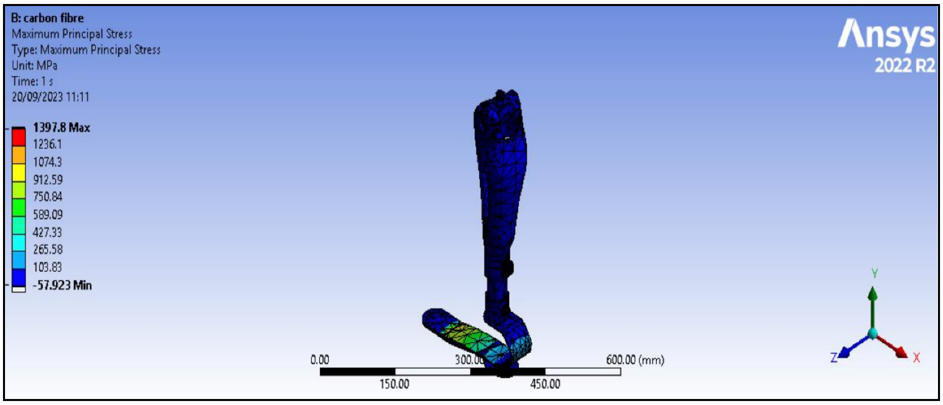


**Fig 30: Material 1: Carbon fibre maximum principal stress**

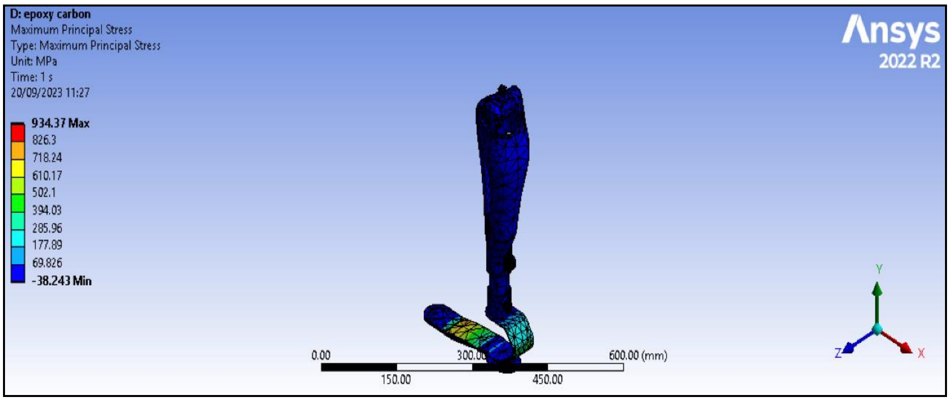


**Fig 31: Material 2: Epoxy carbon woven maximum principal stress**

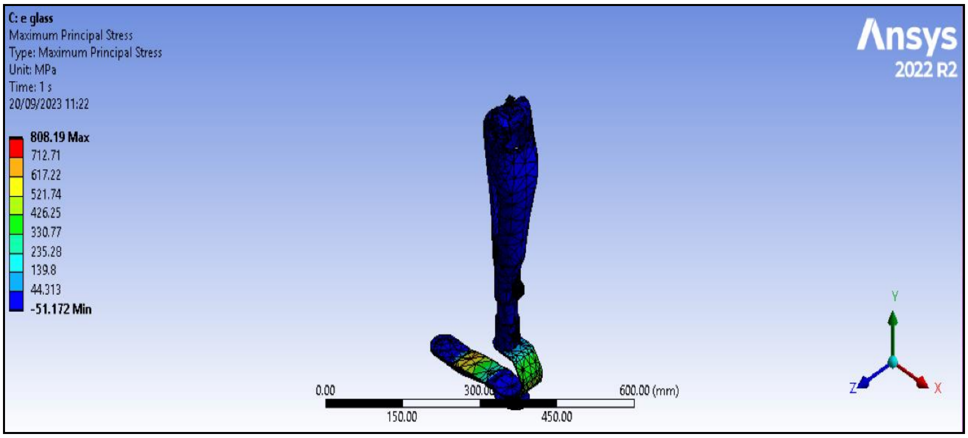


**Fig 32: Material 3: E-glass maximum principal stress**

## 5. Conclusions and Future Pathways

Comprehensive 3-D static structural finite element simulations have been described using ANSYS APDL/WORKBENCH for a robust geometry resembling a lower limb prosthetic inspired by the "Sara Diogo" design [14]. Carbon fibre, Epoxy Carbon Woven Prepreg and E-Glass composite materials have been assessed for structural performance. SOLIDWORKS software has been deployed to create a 3-dimensional prosthetic geometry. Appropriate loading conditions have been prescribed including self-weight and human body average weight. Static stress analysis simulations are conducted for different materials. Mesh independence tests have also been conducted. Equivalent elastic (Von Mises) stress, equivalent strain, maximum principal stress and total deformation plots are presented for all three composite materials examined. The main findings from the ANSYS simulations can be crystallized as follows:

(i)Carbon fibre is justifiably one of the most commonly used composites for making prosthetic limbs globally. As presented in the results, carbon fibre is the structurally best material in terms of resilience and durability and subsequently would be the most appropriate choice for a prosthetic leg. It provides the highest stress values without undergoing plastic deformation, meaning that it can be put through more physical exertion by the user.

(ii)Whilst carbon fibre presents itself as the best option for the physical properties, there are still numerous other factors to take into account when drawing conclusions. These include cost, availability, and longevity, as well as weight and adaptability. Overall, carbon fibre is one of the easier composites to acquire due to the widespread use of it across a number of different industries, including aeroplane manufacturing, cars, mobile devices, even sports equipment such as hockey sticks and golf clubs. Whilst carbon fibre was originally more costly and still is in comparison to materials such as structural steel and aluminium, the lightweight properties and durability outweigh any negativity surrounding the cost. The concept of no yield strength due to the ability of the material to undergo high stress before any plastic deformation almost instantly puts it ahead of metallic materials. The same can also be said of the other composites i.e. Epoxy Carbon Woven Prepreg and E-Glass composite. As these materials deform much easier than carbon fiber, they are less reliable and are also required to be replaced much sooner. This is a large setback, as prosthetics are custom-made and require considerable durability for the user comfort to be sustained.

(iii) In addition, the process of producing bespoke prosthetics is strenuous and time-consuming. Therefore, the less often the prosthetic device requires maintenance (to say nothing of extreme scenarios where full replacement may be warranted), time saving, cost minimization and user comfort will be optimized. In the biomechanical industry, reproducibility in manufacturing and quick modifications for different clients is also critical.

(iv) Due to the fact that all of the composites studied here have benefits surrounding lifespan and weight, in comparison to some metals, for example, determining the most suitable material must be done by drawing comparisons in physical properties, as already discussed. Whilst carbon fibre is the most obvious choice for composite to use in prosthetic devices, that is not to say the other materials that have been tested in this project do not have potential to be used, this is supported by the fact that they are used by a small handful of manufacturers for key components of prosthetics. The three materials do share similarities and therefore this deduction is reasonable. Future directions for refining the present ANSYS simulations include:

(i)Firstly, a key development is the deployment of nanocomposites for prosthetics [30], which offer enhanced durability, comfort, ecological computability and other advantages. Nanocomposites are also identified as improved and effectual biomaterials in the preparation of various prosthetic devices. In prosthetic applications, nanocomposites are used in orthopaedic prosthetics, dental prosthetics, maxillofacial prosthetics, cardiac prosthetics, etc. Future studies could examine hybrid nanocomposite and traditional composite designs different components of the lower limb prosthetic. Involving all 3 composites and special nanocomposites for particular high stress concentration zones would optimize the strengths and durability. Additionally, one could explore incorporating some metals (e.g. chromium and titanium) for elements such as screws and joints.

(ii)The current base study was confined to static stress analysis. Future work could explore dynamic forces associated with actual gait (walking), twisting (torsion) and asymmetric bending [31]. Additionally, conducting a study of different forces being applied to the prosthetic would provide an insight into the potential weight limits of the materials. This would benefit the industry, as from the case study, it has been established that many prosthetic devices have maximum weight limits. Whilst most of these limits exceed average weights it is important that prosthetics can also withstand extreme forces associated with physical, especially for limbs designed for outdoor and extreme sports, and various occupations. This would also extend the applicability of robust prosthetics to a much wider client base.

(iii)Interfacial contact mechanics could also be examined which is critical in the socket zone and has a great influence on user comfort. Contact mechanics [32, 33] in prosthetic modelling evaluates the pressure, friction, and slip at the interface between the residual limb (soft tissue) and the prosthetic socket to prevent tissue damage. In ANSYS Workbench [34], this requires nonlinear contact formulations, hyper-elastic material properties, and specific boundary conditions to simulate realistic donning and load-bearing states.

(iv) Appropriate adjustments could be made to the geometric model to de-bulk the model. This would involve finite element structural optimization [35, 36] and would make the prosthetic slightly lighter, adding ease for the user. Additionally, the connections to the residuum could also be improved, or adjusted to allow other areas of the limb to be fixed and provide a different view of weight distribution.

Efforts in all four directions are currently underway and will be reported imminently.

**Appendix A.**

Finite element analysis (FEA) is a mathematical simulation providing approximate solutions to multi-physical problems. There are many commercial softwares which are used in modern engineering simulation including ADINA, COMSOL, OPENFOAM, NASTRAN, ABAQUS etc. These softwares generally feature numerical "solver" formulations based on the most versatile numerical method known as the finite element method (FEM). These codes can simulate structural, thermal and fluid dynamic phenomena. To properly interpret the output of these softwares i.e. contour plots of deformation, equivalent stress/strain etc, it is essential to appreciate the mathematical methodology underlying the codes. In this study, ANSYS was deployed. ANSYS Workbench uses advanced finite element formulations for stress analysis. These are generally linear. Here aspects of the formulations employed are summarized. These approaches are utilized for all the 3-dimensional simulations [34].

### A1. Combined Stresses and Strains

When a model has only one functional direction of strains and stress (e.g., LINK8), comparison with an allowable value is straightforward. However, when there is more than one component, the components are normally combined into one number to allow a comparison with an allowable.

### A2. Combined Strains

The principal strains are calculated from the strain components by the 3-D matrix equation:

$$\begin{vmatrix} \varepsilon_x - \varepsilon_o & \frac{1}{2}\varepsilon_{xy} & \frac{1}{2}\varepsilon_{xz} \\ \frac{1}{2}\varepsilon_{xy} & \varepsilon_y - \varepsilon_o & \frac{1}{2}\varepsilon_{yz} \\ \frac{1}{2}\varepsilon_{xz} & \frac{1}{2}\varepsilon_{yz} & \varepsilon_z - \varepsilon_o \end{vmatrix} = 0 \tag{A1}$$

Here $\varepsilon_o$ = principal strain (3 values). The **three principal strains** are labelled $\varepsilon_1$ , $\varepsilon_2$, and $\varepsilon_3$ (output as 1, 2, and 3 with strain items such as EPEL). The **principal strains** are ordered so that $\varepsilon_1$ is the most positive and $\varepsilon_3$ is the most negative. The strain intensity $\varepsilon_1$ (output as INT with strain items such as EPEL) is the largest of the absolute values of $\varepsilon_1 - \varepsilon_2$, $\varepsilon_2$ - $\varepsilon_3$, or $\varepsilon_3$ - $\varepsilon_1$. That is:

$$\varepsilon_I = \mathrm{MAX}\left(|\varepsilon_1 - \varepsilon_2|, |\varepsilon_2 - \varepsilon_3|, |\varepsilon_3 - \varepsilon_1|\right) \tag{A2}$$

The **von Mises** or equivalent strain $\varepsilon_e$ (output as EQV with strain items such as EPEL) is computed as:

$$\varepsilon_e = \frac{1}{1+\nu'}\left(\frac{1}{2}\left[(\varepsilon_1 - \varepsilon_2)^2 + (\varepsilon_2 - \varepsilon_3)^2 + (\varepsilon_3 - \varepsilon_1)^2\right]\right)^{\frac{1}{2}} \tag{A3}$$

**A3. Combined Stresses**

The principal stresses ($\sigma_1$, $\sigma_2$, $\sigma_3$) are calculated from the stress components by the cubic equation:

$$\begin{vmatrix} \sigma_x - \sigma_o & \sigma_{xy} & \sigma_{xz} \\ \sigma_{xy} & \sigma_y - \sigma_o & \sigma_{yz} \\ \sigma_{xz} & \sigma_{yz} & \sigma_z - \sigma_o \end{vmatrix} = 0 \tag{A4}$$

Here $\sigma_o$ =Principal stress (3 values). The three principal stresses are labelled $\sigma_1$, $\sigma_2$, and $\sigma_3$ (output quantities S1, S2, and S3). The principal stresses are ordered so that $\sigma_1$ is the most positive (tensile) and $\sigma_3$ is the most negative (compressive).

The stress intensity $\sigma_I$ (output as SINT) is the largest of the absolute values of ($\sigma_1$- $\sigma_2$), ($\sigma_2$- $\sigma_3$), or ($\sigma_3$ - $\sigma_1$). That is:

$$\sigma_I = \mathrm{MAX}\left(|\sigma_1 - \sigma_2||\sigma_2 - \sigma_3||\sigma_3 - \sigma_1|\right) \tag{A5}$$

The von Mises or equivalent stress $\sigma_e$ (output as SEQV) is computed as:

$$\sigma_e = \sqrt{\left[\frac{1}{2}[(\sigma_1 - \sigma_2)^2 + (\sigma_2 - \sigma_3)^2 + (\sigma_3 - \sigma_1)^2\right]]} \tag{A6}$$

or

$$\sigma_e = \left(\frac{1}{2}[(\sigma_x - \sigma_y)^2 + (\sigma_y - \sigma_z)^2 + (\sigma_z - \sigma_x)^2 + 6\left(\sigma_{xy}^2 + \sigma_{yz}^2 + \sigma_{xz}^2\right)]\right)^{\frac{1}{2}} \tag{A7}$$

When $\nu' = \nu$ (input as PRXY or NUXY on MP command), the equivalent stress is related to the equivalent strain through:

$$\sigma_e = E\varepsilon_e \tag{A8}$$

Here E= Young's modulus in N/m$^2$ (input as EX on MP command)

**A4. Failure Criteria**

ANSYS employs failure criteria to assess the possibility of failure of a material. Doing so allows the consideration of orthotropic materials, which might be much weaker in one direction than another. Failure criteria are available in POST1 for all plane, shell, and solid structural elements (using the FC family of commands). Possible failure of a material can be evaluated by up to six different criteria, of which three are pre-defined. They are evaluated at the top and bottom (or middle) of each layer at each of the in-plane integration points.

The failure criteria are outlined briefly below:

**A4-1 Maximum Strain Failure Criteria**

$$\xi_1^f = \text{maximum of} \begin{cases} \dfrac{\varepsilon_{xt}}{\varepsilon^f{}_{xt}} \; or \; \dfrac{\varepsilon_{xc}}{\varepsilon^f{}_{xc}} \text{ whichever is applicable} \\ \dfrac{\varepsilon_{yt}}{\varepsilon^f{}_{yt}} \; or \; \dfrac{\varepsilon_{yc}}{\varepsilon^f{}_{yc}} \text{ whichever is applicable} \\ \dfrac{\varepsilon_{zt}}{\varepsilon^f{}_{zt}} \; or \; \dfrac{\varepsilon_{zc}}{\varepsilon^f{}_{zc}} \text{ whichever is applicable} \\ \dfrac{\left|\varepsilon_{xy}\right|}{\varepsilon^f{}_{xy}} \\ \dfrac{\left|\varepsilon_{yx}\right|}{\varepsilon^f{}_{yx}} \\ \dfrac{\left|\varepsilon_{xz}\right|}{\varepsilon^f{}_{xz}} \end{cases} \tag{A9}$$

Where:

$\xi_1^f$ = value of maximum strain failure criterion

$$\varepsilon_{xt} = \begin{cases} 0 \\ \quad \text{whichever is greater} \\ \varepsilon_x \end{cases}$$

$\varepsilon_x =$ strain in layer x-direction

$$\varepsilon_{xc} = \begin{cases} \varepsilon_x \\ \quad \text{whichever is lesser} \\ 0 \end{cases}$$

$\varepsilon_{xt}^f$ = failure strain in layer x-direction in tension.

**A4-2 Maximum Stress Failure Criteria**

$$\sigma_1^f = \text{maximum of} \begin{cases} \dfrac{\sigma_{xt}}{\sigma^f{}_{xt}} \; or \; \dfrac{\sigma_{xc}}{\sigma^f{}_{xc}} \text{ whichever is applicable} \\ \dfrac{\sigma_{yt}}{\sigma^f{}_{yt}} \; or \; \dfrac{\sigma_{yc}}{\sigma^f{}_{yc}} \text{ whichever is applicable} \\ \dfrac{\sigma_{zt}}{\sigma^f{}_{zt}} \; or \; \dfrac{\sigma_{zc}}{\sigma^f{}_{zc}} \text{ whichever is applicable} \\ \dfrac{\left|\sigma_{xy}\right|}{\sigma^f{}_{xy}} \\ \dfrac{\left|\varepsilon_{yx}\right|}{\sigma^f{}_{yx}} \\ \dfrac{\left|\sigma_{xz}\right|}{\sigma^f{}_{xz}} \end{cases} \tag{A10}$$

Where:

$\sigma_1^f$ = value of maximum stress failure criterion.

$$\sigma_{xt} = \begin{cases} 0 \\ & \text{whichever is greater} \\ \sigma_x \end{cases}$$

$\sigma_x =$ Stress in layer x-direction

$$\sigma_{xc} = \begin{cases} \sigma_x \\ & \text{whichever is lesser} \\ 0 \end{cases}$$

$\sigma_{xt}^f =$ failure stress in layer x-direction in tension.

**A5. 3-D ANSYS solid finite elements**

For 3-D stress analysis, 3-D finite elements must be used. A three-dimensional (3D) solid element can be considered to be the most general of all solid finite elements since all the field variables are dependent on all three Cartesian coordinates, x, y and z. The basic concepts, procedures and formulations for 3D solid elements can also be found in Bathe [36]. We deploy **tetrahedral** (pyramid) elements with four nodes and four surfaces. A tetrahedron element has four nodes, each having three DOFs (u, v and w), making the total DOFs in a tetrahedron element equal to twelve. All structural meshes are built for the prosthetic using 3-D tetrahedron elements ("tets"). The flexibility or compliance matrix, $[D]^{-1}$, in a columnized normal format is shown as:

$$[D]^{-1} = \begin{bmatrix} \frac{1}{E_x} & -\frac{v_{xy}}{E_y} & \frac{-v_{xz}}{E_z} & 0 & 0 & 0 \\ -\frac{v_{yx}}{E_x} & \frac{1}{E_y} & \frac{-v_{yz}}{E_z} & 0 & 0 & 0 \\ -\frac{v_{zx}}{E_x} & -\frac{v_{zy}}{E_y} & \frac{1}{E_z} & 0 & 0 & 0 \\ 0 & 0 & 0 & \frac{1}{G_{xy}} & 0 & 0 \\ 0 & 0 & 0 & 0 & \frac{1}{G_{yz}} & 0 \\ 0 & 0 & 0 & 0 & 0 & \frac{1}{G_{xz}} \end{bmatrix} \tag{A11}$$

Where:

$E_x$ = Young's modulus in the x direction

$v_{xy}$ = Minor Poisson ratio

$\bar{v}_{xy}$ = Major Poisson ratio

$G_{xy}$ = Shear modulus in the x, y plane.

The $[D]^{-1}$ matrix must be positive and assumed to be symmetric. The element integration point strains and stresses are computed by combining the following two equations:

$$\{\varepsilon^{el}\} = [B]\{u\} \tag{A12}$$

$$\{\sigma\} = [D]\{\varepsilon^{el}\} \tag{A13}$$

Here:

$\{\varepsilon^{el}\}$ = Elastic strain vector

$[B]$ =Strains-displacement matrix evaluated at integration point

$\{u\}$ = Nodal displacement vector

$\{\sigma\}$ = Stress vector

$[D]$ = Elastic or elastic stiffness matrix.

**References**


[1] L. Paternò, M. Ibrahimi, E. Gruppioni, A. Menciassi, L. Ricotti, Sockets for limb prostheses: a review of existing technologies and open challenges, *IEEE Transactions on Biomedical Engineering,* Vol. 65, No. 9, pp. 1996-2010, 2018.

[2] J. Andrysek, Lower-limb prosthetic technologies in the developing world: A review of literature from 1994–2010, *Prosthetics and Orthotics International,* Vol. 34, No. 4, pp. 378-398, 2010.

[3] I. Neelen, B. van der Windt, M. J. Major, G. Smit, State of the art of lower limb prosthesis simulators: A literature review, *Wearable technologies,* Vol. 7, pp. e2, 2026.

[4] C. Bruxelas, ISO 10328. Prosthetics. Structural testing of lower-limb prostheses. Requirements and test methods, *Especifica os procedimentos para testes de resistência estática e cíclicos sobre próteses de membros inferiores. International Organization for Standardization, Bruxelas*, pp. 136, 2006.

[5] J. J. Singh, J. S. Mehta, R. Kumar, G. Sapra, FEA simulations of lower limb prosthetics, in *Proceeding of,* IOP Publishing, pp. 012030.

[6] Z. Shuxian, Z. Wanhua, L. Bingheng, 3D reconstruction of the structure of a residual limb for customising the design of a prosthetic socket, *Medical Engineering & Physics,* Vol. 27, No. 1, pp. 67-74, 2005.

[7] F. M. Rohjoni, M. N. A. Ab Patar, J. Mahmud, H. Lee, A. Hanafusa, Finite element analysis of a transtibial prosthetic during gait cycle, *International Journal of Mechanical Engineering and Robotics Research,* Vol. 9, No. 5, pp. 764-70, 2020.

[8] P. Prochor, E. Sajewicz, A comparative analysis of standardised threads for use in implants for direct skeletal attachment of limb prosthesis: a finite element analysis, *Applied Bionics and Biomechanics,* Vol. 2019, No. 1, pp. 8027064, 2019.

[9] W. C. Lee, M. Zhang, X. Jia, J. T. Cheung, Finite element modeling of the contact interface between trans-tibial residual limb and prosthetic socket, *Medical Engineering & Physics,* Vol. 26, No. 8, pp. 655-662, 2004.

[10] J. W. Steer, P. R. Worsley, M. Browne, A. Dickinson, Key considerations for finite element modelling of the residuum–prosthetic socket interface, *Prosthetics and Orthotics International*, pp. 0309364620967781, 2021.

[11] I. Boudjemaa, A. Albedah, A. Sahli, B. A. B. Bouiadjra, S. Benbarek, Innovative stress-responsive liner design for lower limb disability, *Journal of Disability Research,* Vol. 3, No. 8, pp. 20240098, 2024.

[12] A. A. Cherif, M. Abdelmadjid, Z. M. El Sallah, B. Ali, M. Yaylacı, S. Abderahmane, M. E. Özdemir, A. Dizdar, E. U. Yaylacı, Y. Güvercin, Comparative study by FEM of different liners of a transfemoral amputated lower limb, *Scientific Reports,* Vol. 15, No. 1, pp. 31878, 2025.

[13] C. Barattini, L. Dimauro, A. D. Vella, A. Vigliani, Dynamic analysis of a high-performance prosthetic leg: experimental characterisation and numerical modelling, *Applied Sciences,* Vol. 13, No. 20, pp. 11566, 2023.

[14] S. Diogo. *Sara Diogo*, Accessed; https://grabcad.com/sara.diogo.

[15] Össur. *Pro-Flex XC Torsion*, Accessed; https://media.ossur.com/ossur-dam/image/upload/product-documents-global/Pro_Flex_XC_Torsion_gb_en_PN20221.pdf.

[16] Steeper Group. *DynAdapt Foot - Prosthetic Feet*, Accessed; https://www.steepergroup.com/prosthetics/lower-limb-prosthetics/feet/dynadapt/.

[17] Ottobock. *Maverick Comfort AT*, Accessed; https://www.ottobock.com/en-gb/product/F22-61066.

[18] G. Nawel, S. Abderahmane, M. Abdelmadjid, Z. M. E. Sallah, M. Yaylacı, Ş. Öztürk, B. Ismail, E. U. Yaylacı, A. Dizdar, Y. Güvercin, Biomechanical evaluation of a lower-limb implant model under gait and stumbling conditions using finite element analysis, *Scientific Reports,* Vol. 15, No. 1, pp. 41443, 2025.

[19] K. Carroll, Lower extremity socket design and suspension, *Physical Medicine and Rehabilitation Clinics,* Vol. 17, No. 1, pp. 31-48, 2006.

[20] O. A. Bég, S. Kuharat, T. A. Bég, J. Pattison, A. Kadir, H. J. Leonard, W. Jouri, *Two-Way Fluid-Structure Interaction Hydroelastic Simulation of Vibrating Membranes with Applications in Marine Renewable Wave Power*, in: *Eco-Materials and Green Energy for a Sustainable Future*, Eds., pp. 295-329: CRC Press, 2024.

[21] K. Gupta, S. Kuharat, O. Anwar Bég, Thermo-Mechanical Assessment of Clay-Based Barriers for Nuclear Waste Repositories using Finite Element Analysis, *Journal of Dynamics, Energy and Utility,* Vol. 2, No. 1, pp. 9-24.

[22] C. Amaze, S. Kuharat, O. Anwar Bég, A. Kadir, W. Jouri, T. A. Bég, Finite element stress analysis and topological optimization of a commercial aircraft seat structure, *European Mechanical Science,* Vol. 8, No. 2, pp. 54-70, 2024.

[23] J. Buxton, O. Anwar Bég, T. A. Beg, M. Bhatti, S. Kuharat, A. Kadir, W. S. Jouri, Finite element stress analysis of a bumblebee-inspired micro air vehicle (MAV) wing, *Journal of Mechanics in Medicine and Biology*, pp. 2650059, 2026.

[24] A. Kadir, O. Anwar Bég, M. El Gendy, T. A. Bég, M. Shamshuddin, Computational fluid dynamic and thermal stress analysis of coatings for high-temperature corrosion protection of aerospace gas turbine blades, *Heat Transfer—Asian Research,* Vol. 48, No. 6, pp. 2302-2328, 2019.

[25] O. Anwar Bég, B. Islam, M. Shamshuddin, T. A. Bég, Computational fluid dynamics analysis of moisture ingress in aircraft structural composite materials, *Arabian Journal for Science and Engineering,* Vol. 44, No. 9, pp. 7809-7831, 2019.

[26] M. E. GENDY, O. A. Bég, A. Kadir, M. Islam, D. Tripathi, Computational fluid dynamics simulation and visualization of Newtonian and non-Newtonian transport in a peristaltic micro-pump, *Journal of Mechanics in Medicine and Biology,* Vol. 21, No. 08, pp. 2150058, 2021.

[27] Y.-C. Fung, 2013, *Biomechanics: mechanical properties of living tissues*, Springer Science & Business Media,

[28] A. M. Grabowski, S. D'Andrea, Effects of a powered ankle-foot prosthesis on kinetic loading of the unaffected leg during level-ground walking, *Journal of neuroengineering and rehabilitation,* Vol. 10, No. 1, pp. 49, 2013.

[29] A. Javidinejad, 2023, *Essentials of Mechanical Stress Analysis*, CRC Press,

[30] M. S. Hasnain, S. A. Ahmad, M. A. Minhaj, T. J. Ara, A. K. Nayak, *Nanocomposite materials for prosthetic devices*, in: *Applications of Nanocomposite Materials in Orthopedics*, Eds., pp. 127-144: Elsevier, 2019.

[31] J. Schuy, N. Stech, G. Harris, P. Beckerle, S. Zahedi, S. Rinderknecht, A prosthetic shank with adaptable torsion stiffness and foot alignment, *Frontiers in Neurorobotics,* Vol. 14, pp. 23, 2020.

[32] F. Naghdbishi, A. Ghouchani, F. Safshekan, K. Ghayyad, A. R. Kachooei, Effects of prosthesis shape and material on the contact mechanics of elbow joints following radial head arthroplasty: an in-silico investigation, *Archives of Bone and Joint Surgery,* Vol. 13, No. 8, pp. 497, 2025.

[33] W. Cui, X. Zhang, W. Chen, J. Qiu, Investigation into the analysis method for assessing contact stress in joint prosthesis, *Medicine in Novel Technology and Devices,* Vol. 22, pp. 100299, 2024.

[34] I. ANSYS, *ANSYS Mechanical Theory Manual*, ANSYS, Inc., Lebanon, New Hampshire, USA, pp. 2022.

[35] T. E. Bountourelis, N. Kladovasilakis, K. Tsongas, P. Kyratsis, D. Tzetzis, Finite element analysis and topology optimization of a high-performance lower prosthetic limb, *International Journal of Modern Manufacturing Technologies (IJMMT),* Vol. 15, No. 1, pp. 148, 2023.

[36] K. J. Bathe, 1996, *Finite Element Procedures*, Prentice Hall, Englewood Cliffs, New Jersey, USA